Diameter-Selective Dispersion of Carbon Nanotubes *via* Polymers: A Competition between Adsorption and Bundling

Hongliu Yang,[*,†] Viktor Bezugly,[†,‡] Jens Kunstmann,[†,§] Arianna Filoramo,[⊥] and Gianaurelio Cuniberti[†,‡,∥]

[†]Institute for Materials Science and Max Bergmann Center of Biomaterials (IfWW & MBZ), [‡]Center for Advancing Electronics Dresden (cfAED), [§]Theoretical Chemistry (TC), Department of Chemistry and Food Chemistry, and [∥]Dresden Center for Computational Materials Science (DCCMS), TU Dresden, 01062 Dresden, Germany and [⊥]DSM/IRAMIS/NIMBE/LICSEN, CEA de Saclay, 91191 Gif sur Yvette, France

ABSTRACT The mechanism of the selective dispersion of single-walled carbon nanotubes (CNTs) by polyfluorene polymers is studied in this paper. Using extensive molecular dynamics simulations, it is demonstrated that diameter selectivity is the result of a competition between bundling of CNTs and adsorption of polymers on CNT surfaces. The preference for certain diameters corresponds to local minima of the binding energy difference between these two processes. Such minima in the diameter dependence occur due to abrupt changes in the CNT's coverage with polymers, and their calculated positions are in quantitative agreement with preferred diameters reported experimentally. The presented approach defines a theoretical framework for the further understanding and improvement of dispersion/extraction processes.

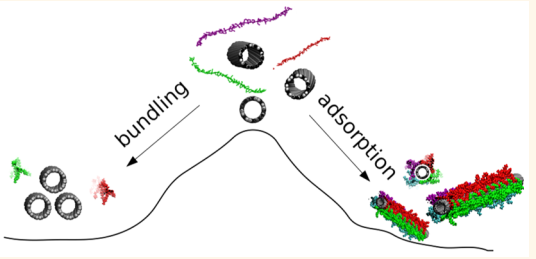

KEYWORDS: carbon nanotubes · diameter selectivity · polymer adsorption · binding energy · molecular dynamics · surface coverage

Since their discovery, single-walled carbon nanotubes (CNTs) have attracted major research interest due to their extraordinary mechanical, chemical, and electronic properties.[1] They are metallic or semiconducting depending on their chirality, and as-synthesized material is normally a mixture of both types. For many applications, however, purified samples of only a certain type are in high demand. Purified semiconducting tubes are required, for instance, to achieve a large on/off ratio and high carrier mobility in thin-film field-effect transistors[2−7] and high power conversion efficiency for photovoltaics.[8,9] Moreover, for optoelectronic applications working in a specific wavelength range, the sorting of semiconducting CNTs according to diameter is of great importance.

In view of such demands, methods for the selective synthesis of CNTs of a certain electronic type or chiralites have been developed.[10,11] A low-cost mass production of selected CNTs is yet to be achieved, however, and postsynthesis methods are often relied on.[12] A promising postsynthesis selection method discovered recently is based on the physisorption of polymers on the surface of CNTs, which has the advantage of leaving the electronic properties of the CNT nearly unperturbed.[12] There is a relatively long history of using polymers to disperse CNTs in aqueous or organic solutions.[13,14] A recent finding is that, by using suitable polymers, CNTs can be selectively dispersed either for a specific diameter range or for certain chiral angles.[12] Among those tested, the π-conjugated polymer group of polyfluorene derivatives shows the ability to selectively disperse semiconducting CNTs.[15−23] In particular, the dioctyl-substituted polyfluorene (PFO) used with toluene as solvent prefers to disperse small-diameter semiconducting nanotubes with chiral angles larger than about 20°.[15] With longer side chains, larger-diameter tubes can be dispersed but the chiral angle preference is gradually lost.[6,20] More recently, copolymers of polyfluorene with anthracene or pyridine groups were found

* Address correspondence to hong-liu.yang@tu-dresden.de.

Received for review May 20, 2015 and accepted August 13, 2015.

Published online August 13, 2015
10.1021/acsnano.5b03051

to selectively disperse large-diameter semiconducting nanotubes with high purity and high yields.[21,22] This fits well with the need to fabricate photoelectronic devices working in the infrared wavelength range.[24] Large-diameter nanotubes also benefit from a diminishing contact resistance and higher carrier mobilities. Purified semiconducting CNTs have been used to fabricate high-performance field-effect transistors with high carrier mobilities and large on−off ratios.[3−7]

Intensive experimental and numerical works have been undertaken to study the conformation of polymers adsorbed on the CNT surface. For DNAs and some biomacromolecules,[25] which prefer to take a helical conformation even in the free state, a helically wrapped configuration on CNT was naturally expected. Studies on the adsorption conformation of linear conjugated polymers are less conclusive. For instance, poly(arylene ethynylene)s (PAEs) were found to align linearly along the CNT when dispersed with toluene.[26] The similar poly(*p*-phenylene ethynylene) polymer, poly[*p*-2,5-bis(3-propoxysulfonic acid sodium salt)-phenylene]ethynylene, was found to form helically wrapped structures in an aqueous dispersion.[27,48] Imaged *via* scanning electron microscopy, it was shown that when dispersed in chloroform, poly(3-hexylthiophene) (P3HT) forms a helically wrapped structure on the surface of multiwalled CNTs.[28] Recently, regioregular poly(3-alkylthiophene)s (rr-P3ATs) were used with toluene as solvent to enrich semiconducting CNTs, and molecular dynamics (MD) simulations showed that P3ATs take quasi-linear conformations, as adsorbed on CoMoCAT CNTs.[35] In 2014, Shea *et al.* reported the first experimental study on the adsorption configuration of PFOs on CNTs by using photoluminescence energy transfer and anisotropy measurements.[33] Their data, however, are open to interpretation.[34]

In the past, efforts were also made to theoretically explain the selection mechanism. For DNAs, the intrinsic helical nature was believed to play a crucial role in their selective adsorption on CNTs.[25] For aromatic polymers, Nish *et al.*[15] found that PFOs on CNT surfaces form *n*-fold symmetric structures with their backbones aligned along the tube axis. The magnitude of the binding energy between CNTs and polymers was shown to increase with the tube diameter, a trend that was later confirmed by several authors.[18,20,23] If the stability of adsorption complexes, as indicated by the binding energy, would determine the dispersibility of CNTs, the above results[15,18,20,23] would imply that large-diameter CNTs are more easily dispersed than small-diameter ones. This, however, is in contradiction to experimental observations that PFO prefers to disperse small-diameter CNTs.[15,18,23] Furthermore, helically wrapped PFO structures on CNTs were used to explain the chirality preference of PFO.[17] We will show below, however, that such helical structures are not dynamically stable. Recently, a coarse-grained model was developed and used together with statistical mechanical arguments to explain the diameter preference of several pyridine-containing copolymers.[22] However, it is unclear how well the method can be transferred to other systems. Despite these advances, it is fair to say that a thorough understanding of the diameter and chirality selectivity of the polymer adsorption method is still lacking.

RESULTS AND DISCUSSION

This article focuses on understanding the diameter selectivity of the polymer adsorption method since the band gap and related electronic/optical properties of semiconducting CNTs are mainly determined by the diameter.[29] In particular, we propose that diameter selectivity results from a competition between the adsorption of polymers on the CNT surface and the bundling of individual CNTs (see Figure 1). Our results on four relevant polymers are in excellent agreement with experimentally observed diameter preferences[15,21,22] and, thus, resolve a controversy on the nature of the mechanism that underlies the diameter selection process. Despite the complexity of the competitive dispersion of CNTs, the success of our simple energetic model regarding diameter selectivity relies on its correct representation of some key factors including steric effects and coverage.

Simulations. To study the CNT dispersion process, we performed classical MD simulations using force fields. Tip sonication treatment is known to generate high, local energy densities that break bundles into individual CNTs.[30,31] For the dilute polymer concentrations used in typical dispersion processes, the polymers exist as individual molecules.[32] Therefore, isolated, individual CNTs and polymers were assumed as the initial configuration. Solvent molecules of toluene were usually not explicitly included here. We tested that their inclusion did not significantly change the results but mostly slowed down the adsorption dynamics. Four representative types of polymers were considered in this study: the homopolymer of polyfluorene with side-chain

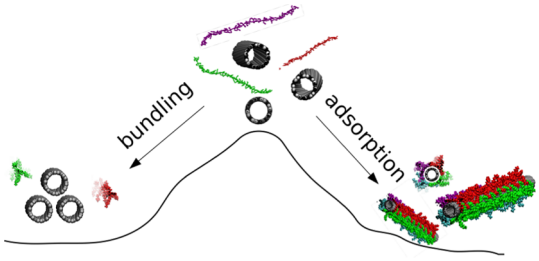

Figure 1. Proposed mechanism of diameter-selective dispersion: a competition between bundling of CNTs and adsorption of polymers on the surface of CNTs. The initial state of the process, given by individual CNTs and individual polymers, is a transition state (on the top of a potential energy hill) created by sonication.

length C8 (PFO) or C6 (PFH) and copolymers with the anthracene group poly[(9,9-dihexylfluorenyl-2,7-diyl)-*co*-(9,10-anthracene)] (PFH-A) or pyridine groups poly-[9,9-didodecylfluorene-2,7-diyl-*alt*-pyridine-2,6-diyl] (PFD-Py). The chemical structures of these four polymers are presented in the Supporting Information. Furthermore, 13 CNTs with diameters in the range from 0.8 to 1.4 nm were considered. Such diameters are typically obtained in high-pressure CO conversion (HiPco) or pulsed laser vaporization (PLV) synthesis. Further information on our simulation methods can be found in the Methods section.

Adsorption Complexes. The geometries of adsorption complexes were obtained by MD simulations using many different initial configurations, temperatures, and CNT diameters. The simulations always lead to an almost linear alignment of PFO chains on the CNT surface, even after using initial conditions that promote the formation of helically wrapped structures. Through geometry optimizations, we found that a multitude of such helically wrapped structures,[17] with different pitches and surface coverages, are local minima on the potential energy landscape (see Figures 2a and S2).[34] However, if they were subjected to MD simulations, unwrapping proceeds gradually and, after a sufficiently long run, a linearly aligned structure, as shown in Figure 2b, was always obtained. We conclude that helically wrapped adsorption complexes are metastable.[34]

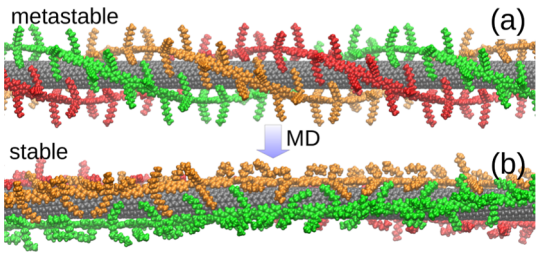

Figure 2. Geometry of adsorption complexes: (a) a helically wrapped configuration is metastable, *i.e.*, a local minimum on the potential energy landscape. (b) Snapshot of the much more stable, linearly aligned configuration of PFO on a (8,6) CNT.

Binding Energy and Stability of Adsorption Complexes. A standard measure used to characterize the stability of the adsorption complex is the binding energy. It is defined as the difference between the potential energy of an adsorption complex and the sum of its constituent molecules. For the adsorption of polymers on the CNT, it reads

$$E^{\text{binding}}_{\text{CNT}-\text{Polymer}} = E_{\text{CNT}-\text{Polymer}} - E_{\text{CNT}} - E_{\text{Polymer}} \quad (1)$$

The binding energy for the adsorption of a single polymer chain on a CNT is shown in Figure 3a. Note that the magnitude of the binding energy increases with the tube diameter, in agreement with previous results.[15,18,20,23] This is caused by a better contact between polymers and CNT owing to the increasingly flatter surface of large-diameter CNTs.[34] The side chain contributes a large part, about two-thirds, to the total binding energy of PFO. Consistently, the binding energy for PFH is smaller due to a shorter side-chain length.[3,20,35] The magnitude of the binding energy of PFH-A is smallest, which means that, for all the tested polymers with similar length, it is the easiest to remove from a CNT surface. This is in qualitative agreement with our recent experimental observation that PFH-A can be washed away from thin films deposited using dispersed CNTs (unpublished results). In contrast, PFO cannot be washed away in the same manner.

Surface Coverage of CNTs by Polymers and Binding Energy of CNT–Polymer Complexes. To avoid the rebundling of CNTs after sonication, it is necessary to sufficiently cover the CNT surface with polymers.

We concentrate here on the situations where there is an excess of polymers and maximal coverage of the CNT surface is expected. Binding energies for the maximal coverage of CNTs by polymers are shown in Figure 3b. Note the discontinuities in the binding energy that are due to a sudden change in the number

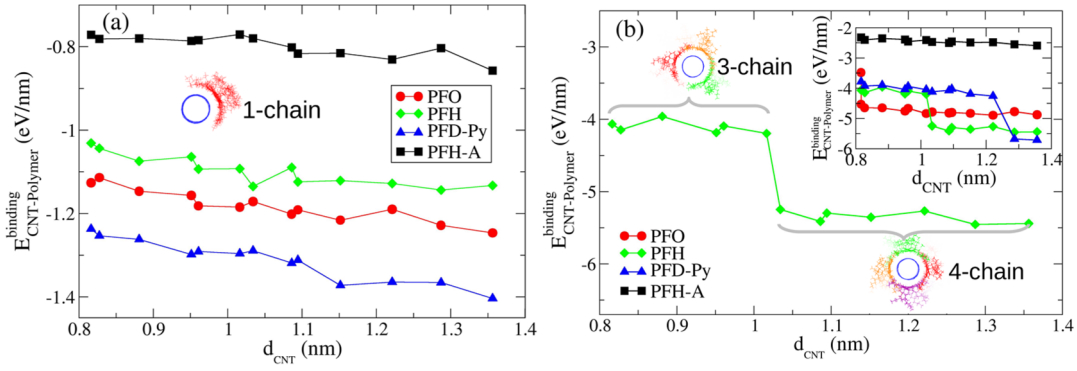

Figure 3. Binding energy $E^{\text{binding}}_{\text{CNT}-\text{Polymer}}$ (eq 1) of adsorption complexes for (a) a single polymer chain and (b) the maximal coverage of the CNT surface. The magnitude of the binding energy increases with the nanotube diameter. Therefore, the binding energy $E^{\text{binding}}_{\text{CNT}-\text{Polymer}}$ alone cannot explain why polymers selectively disperse CNTs with specific diameters. Note the discontinuities of $E^{\text{binding}}_{\text{CNT}-\text{Polymer}}$ in (b) that are due to abrupt changes in the surface coverage of the CNTs.

of polymers needed for maximal surface coverage.[15] The positions of the discontinuities are different from those reported previously in the literature[15,18,20,23] because our MD simulations lead to different surface coverages than the geometry optimizations performed in those works.[34] These discontinuities have a direct relation to the diameter preference of polymers, as will be discussed below.

Polymer-Assisted Dispersion as a Competition between Adsorption and Bundling. The binding energy $E^{\text{binding}}_{\text{CNT-Polymer}}$ alone cannot explain the selectivity of the polymer adsorption method because its magnitude simply increases with the diameter (see Figure 3). This would imply that large-diameter CNTs are more easily dispersed than small-diameter ones. However, this is in clear contrast to the experimental observations discussed above.[15,21] The binding energy between polymer-wrapped CNTs could explain well the polymer-assisted dispersion of CNTs in certain solvents but not the selectivity on CNTs. The key factor for understanding the selection mechanism is competition between the bundling of CNTs on the one hand and the adsorption of polymers on the CNT surface on the other (see Figure 1). This reasoning is based on the observation that CNT dispersions in toluene without polymers are not stable and the CNTs eventually rebundle. For this competition to take place, the initial state to be considered is a transition state consisting of individual polymers and individual CNTs. This transition state is experimentally realized by sonication, an integral work step of all selection methods. Therefore, the selectivity of CNTs is determined by the *difference* between the binding energy for CNT bundling and the binding energy for polymer adsorption, which reads

$$\Delta E^{\text{binding}} = E^{\text{binding}}_{\text{CNT-Polymer}} - E^{\text{binding}}_{\text{CNT-CNT}} \quad (2)$$

Binding Energy of CNT Bundles. As-produced CNTs are normally a mixture of different diameters. This polydisperse nature makes a direct simulation of bundling computationally very expensive. To overcome the difficulties, we first calculated the average pair binding energy $\bar{E}_i$ of the interaction between a CNT of a given diameter and another CNT, arbitrarily selected from a sample of mixed CNTs. It reads

$$\bar{E}_i = \sum_j w_j E_{ij} \quad (3)$$

where E_{ij} is the pair binding energy between CNT species i and j, and w_j is the population weight (abundance) of CNT species j in the sample. As shown in Figure 4a, the magnitude of $\bar{E}_i$ increases with the CNT diameter, due to the increase in the contact area between CNTs. Next, we estimate the average number of neighbors, N_{avg}, of a CNT in bundles. A simple approach would be to ignore the polydispersity and assume that all CNTs have just six neighbors, but our method is to consider the surface of a CNT of a given diameter to be covered by CNTs having the average diameter of the considered sample (*i.e.*, HiPco or PLV). Therefore, the average number of neighbors can be a noninteger. The estimates of N_{avg} for two CNT samples are presented in Figure 4b. Finally, the binding energy for CNT bundling $E^{\text{binding}}_{\text{CNT-CNT}}$ can be calculated as

$$E^{\text{binding}}_{\text{CNT-CNT}} = \bar{E}_i N_{\text{avg}} \quad (4)$$

As shown in Figure 4c for both samples, the magnitude of the binding energy of CNT bundles increases with the CNT diameter.

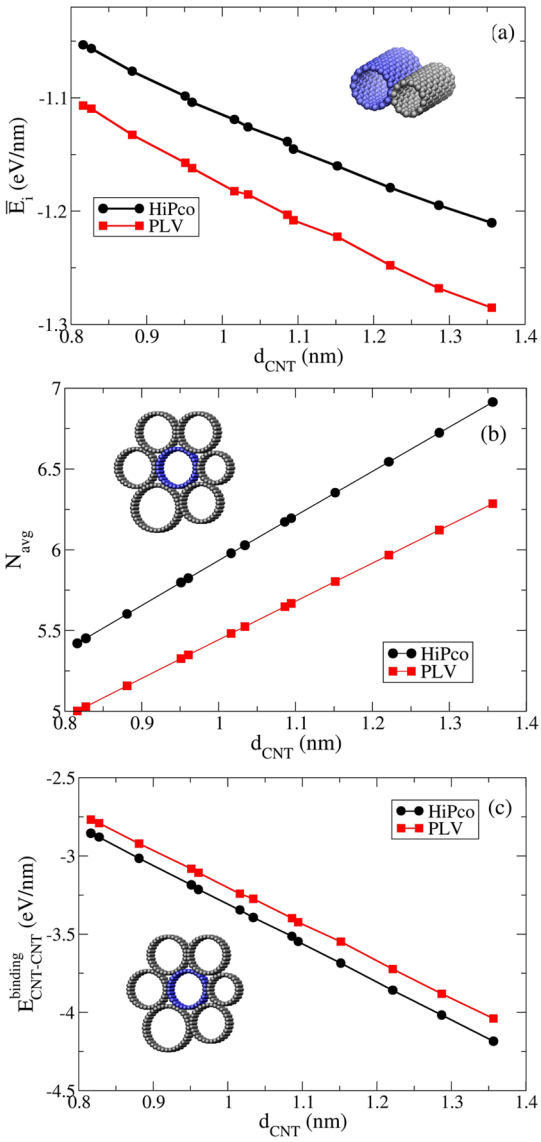

Figure 4. Energetics of CNT bundling: (a) weighted average $\bar{E}_i$ (eq 3) of the pair binding energy of the interaction between a CNT of a given diameter and another CNT, arbitrarily selected from the sample. (b) Average number of neighbors, N_{avg}, of a CNT with a given diameter in a bundle with mixed diameters (fractional numbers are a result of the nonuniform diameter distribution). (c) Binding energy $E^{\text{binding}}_{\text{CNT-CNT}} = \bar{E}_i N_{\text{avg}}$ of CNT bundling. The variation of $E^{\text{binding}}_{\text{CNT-CNT}}$ with the diameter follows the same trend as $E^{\text{binding}}_{\text{CNT-Polymer}}$ in Figure 3, and only the competition between adsorption and bundling leads to selectivity.

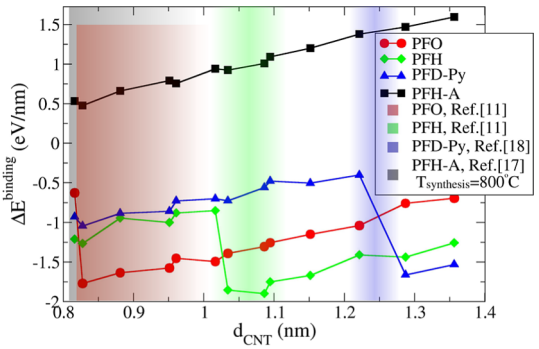

Figure 5. Diameter selectivity as competition between CNT bundling and polymer adsorption. The diameter preferences of specific polymers for HiPco CNTs in our simulations are defined by the minima of the corresponding binding energy difference $\Delta E^{binding}$ (eq 2). They are in excellent agreement with experimental results indicated by the shadowed regions.[15,21,22]

Binding Energy Difference and Diameter Selectivity. As discussed already, for both CNT bundles and CNT−polymer complexes, the magnitude of the binding energy increases with the tube diameter. In the binding energy difference $\Delta E^{binding}$, the two trends nearly compensate for each other and only their competition leads to the preference for certain diameters, which are reflected in the location of the minima of $\Delta E^{binding}$ in Figure 5.

Consider first the adsorption of PFO on HiPco CNTs in Figure 5. Except for the CNT with the smallest diameter, $\Delta E^{binding}$ increases with tube diameter. Since the number of polymers needed for the maximal surface coverage of the CNTs changes from three to four, $E^{binding}_{CNT-Polymer}$ abruptly changes at 0.83 nm (see inset of Figure 3b), causing $\Delta E^{binding}$ to have a minimum at about the same diameter. The behavior of $\Delta E^{binding}$ explains (i) the preference of PFO to disperse HiPco CNTs in the diameter range of 0.8−0.95 nm, a fact that has been repeatedly reported by different groups,[15,18,23] and (ii) why CNTs with diameter smaller than 0.8 nm are not well-dispersed by PFO. These two insights explain the dominance of (8,6) CNTs (d = 0.95 nm) in HiPco CNT dispersions and the elimination of (6,5) CNTs (d = 0.75 nm) in CoMoCAT CNT dispersions.[15]

For PFH, with side chains two carbon atoms shorter than PFO, more polymer chains are needed to cover the surface of a CNT. Therefore, the discontinuity in $\Delta E^{binding}$ is upshifted to 1.03 nm. This explains why, for HiPco CNTs using PFH instead of PFO, the dominant CNTs in the dispersion become (8,7) (d = 1.02 nm) and (9,7) (d = 1.09 nm) (see Figure 1b of Nish *et al.*[15]).

For the copolymer PFD-Py, the minimum of $\Delta E^{binding}$ is about 1.25 nm. This agrees with recent experimental findings that, for HiPco CNTs, PFD-Py prefers to disperse CNTs with diameters of about 1.23 nm (see Figure 1n of Berton *et al.*[22]).

The $\Delta E^{binding}$ of PFH-A increases continuously in the considered diameter range (0.8−1.4 nm), and no minimum is discernible. Mistry *et al.* performed a systematic study on the selectivity of PFH-A on CNTs synthesized *via* laser vaporization of graphite at different temperatures and found that it always prefers to disperse CNTs with the smallest diameters in the sample.[21] The absence of a minimum in that range is again consistent with the experiments, even though the simulations are based on HiPco CNTs. Further discussions on the selectivity of PFH-A can be found in the Supporting Information.

To summarize, for the polymers PFO, PFH, and PFD-Py, the minima of the binding energy difference $\Delta E^{binding}$ match perfectly the experimentally reported diameters that are dominantly dispersed by those polymers. This excellent agreement strongly suggests that the mechanism of diameter selectivity is a competition between CNT bundling and polymer adsorption.

It is interesting to note that the sign of $\Delta E^{binding}$ is negative for PFO, PFH, and PFD-Py. This indicates a preference for the formation of CNT−polymer adsorption complexes over CNT−CNT bundling. Therefore, for long sonication times, single-walled CNTs of all diameters can be dispersed, in principle. With increasing sonication time, the amount of dispersed CNTs will increase and the selectivity will gradually diminish. Therefore, an optimal sonication time should be experimentally determined, providing a compromise between yield and purity. Positive values of $\Delta E^{binding}$ for PFH-A mean that the rebundling should happen more frequently than adsorption, which implies a potential lower yield of the dispersion process using PFH-A.

Note also that, due to the possibility of partial adsorption and other "imperfect" packing configurations, the transition in Figure 3b may turn out to be not so abrupt; see also the radial distribution functions shown in Figure S6 and the corresponding discussions in the Supporting Information. Therefore, in experiments, a range of diameters is often selected by a certain polymer.

One can also view the sonication-assisted dispersion process as a reversible reaction

$$\text{CNT@CNT} + \text{PFO} \rightleftharpoons \text{PFO@CNT} \qquad (5)$$

In this language, the initial configuration of isolated CNTs and polymers corresponds to a transition state, which is achieved with the aid of ultrasonication treatment.[30,31] The adsorption of polymers on the CNT surface and the bundling of CNTs are the rate-determining steps for forward and backward reactions, respectively. The two binding energies are the (negative) activation energies for reactions in the two directions. For this reversible reaction, the binding energy difference only estimates energetic contributions to the reaction rates, neglecting entropic contributions, reaction orders, and the concentrations of the reactants.

The focus of the current study is on the diameter selectivity of CNTs by aromatic polymers. For the chirality selection, the match/mismatch between the

atomic structures of polymers and CNTs will be quite crucial. The popular implementations of van der Waals' interaction, as used here, were found to be unsuitable for this purpose, and the anisotropic intermolecular potentials turn out to be a better alternative.[37] For the sorting of CNTs with respect to electronic properties, *ab initio* quantum simulations with the electronic interactions being included would be more appropriate. All of these issues deserve their own separate publications. The mentioned success of our simple energetic model implies that the key factors determining the diameter selectivity of (semiconducting) CNTs were properly represented. The model can certainly be further improved by including (i) entropy factors for a proper estimate of Gibbs free energy, which is of direct relevance to the reaction kinetics, and (ii) the effect of explicit solvent. Calculations with explicit solvents and estimates of entropic contributions are provided in the Supporting Information.

In conclusion, we explain the diameter selectivity of polymer adsorption methods to be the result of a competition between the bundling of CNTs and the adsorption of polymers on the CNT surface. The preference of certain diameters corresponds to local minima of the binding energy difference between these two processes. Such minima occur due to abrupt changes in the CNT's coverage with polymers at certain diameters. For all tested polymers including two homopolymers of polyfluorene with different side-chain lengths and two copolymers with anthracene or pyridine groups, our simulation results are in excellent agreement with the experimental findings regarding the diameter selectivity. Interestingly, even the influence of a fine-tuning of side-chain length on the selectivity was correctly captured in our method. Our insights resolve a long-standing controversy regarding the understanding of CNT selection schemes and are important for the further development of dispersion/extraction methods; that is, they enable MD simulations to be used for the screening of polymer candidates, tailoring of polymer structures, and obtaining further scientific insights. The proposed mechanism is general enough to be valid for other (sonication-aided) dispersion processes, for instance, the exfoliation of layered materials[36] and the dispersion of CNTs by DNAs and mononucleotides.[25,47−50]

METHODS

The adsorption of polymers on single-walled CNTs and the bundling of CNTs were studied with classical MD simulations by using the CP2K[43] and Gromacs packages.[40] MD simulations were performed in NVT ensemble at $T = 300$ K using the Nose-Hoover or Langevin thermostats. The standard CHARMM force field parameters for the intramolecular interaction[39] were benchmarked against the density functional method (DFT) MD simulations with Grimme dispersion corrections DFT-D3[44] and the BLYP exchange-correlation functional[45] in CP2K and classical MD simulations with the MM3 force field[41] using the Tinker package.[42] The torsion angle parameter, describing among others the twist of the backbones of polymers, was modified to match the results of DFT first-principles MD simulation. The intermolecular interactions include an electrostatic part due to partial charges on atoms and a dispersion force part modeled by a Lennard-Jones potential as usual in standard CHARMM force field implementations.[39]

For the adsorption of polymers on the CNT surface, the polymer backbones were initially aligned parallel to the CNT axis. Multiple chains of polymers were arranged in an *n*-fold symmetric structure surrounding the tube. The initial distance between the backbone and the CNT surface was set to 1−1.5 nm depending on the CNT diameter and the number of polymers. For the binding energy calculation of CNT pairs, the two CNTs were placed in parallel with the initial distance between the surfaces of 0.6 nm. The time step for the integration of Newton's equation of motion was 1 fs. The duration of MD simulations ranged from 1 to 20 ns. For the calculation of thermodynamic averages, the equilibration time, ranging between 0.2 and 2 ns, was not considered. To check the stability of self-constructed helical adsorption structures, geometry optimizations were performed using the CP2K package. The criteria of convergence are 3×10^{-3} Bohr for the geometry change and 4.5×10^{-4} Hartree/Bohr for the change in the force.

It is known that the solvent plays an important role in the selective dispersion of CNTs by polymers.[38] However, here we are interested in studying the effect of different polymers in combination with the same weakly polarized solvent, toluene. Moreover, our tests showed that the explicit inclusion of solvent molecules of toluene in MD simulations did not change the structures of adsorption but significantly slowed the dynamics of the adsorption process. Therefore, to enable MD simulations within reasonable times, solvent molecules were not explicitly included in our production runs. Our additional MD simulations with explicit solvents showed that the adsorption configurations of the polymer backbones and side chains, which are in contact with CNT surface, hardly change with the inclusion of solvents. Only the side chains, which are not in contact with CNT surface, tend to point outward to the solvent instead of folding back and aligning along the CNT surface as in vacuum. The second layer of polymers moves a bit away from the CNT surface. Therefore, with the inclusion of solvents, the values of binding energies may change by some degree, but the surface coverage of CNTs and the related positions of the abrupt changes in Figure 3b will be unaffected. Further details on the effect of explicit solvent can be found in the Supporting Information. Studies showed that a PFO octamer already has the same selectivity as a PFO polymer. Furthermore, the stability of the oligomer−CNT complex increases strongly with the chain length of the oligomer.[46] To meet the capacity of the available computing resources in our simulation, we used 30 nm long polymer chains, which consist of 32, 22, and 30 monomers of PFO/PFH, PFD-Py, and PFH-A, respectively. CNT segments with a length between 30 and 36 nm were used, with their length varying with the chirality.

To obtain the binding energy of a polymer−CNT complex, three MD simulations were performed for the adsorption complex, the isolated CNT, and the polymer. The mean value of the potential energy was determined from the corresponding trajectories, and the binding energy was then calculated. This procedure is different from most cases in the literature where the binding energy was calculated from ($T = 0$ K) single-point calculations of the optimized structures.

It is worth pointing out that, for the adsorption of polymers on a CNT surface, the binding energy can be measured per unit length of a polymer chain or per unit length of CNT covered completely by polymers. The former describes how hard it is to

remove a polymer chain from the CNT surface, while the latter is suitable for characterizing the competition for the adsorption on a CNT surface.

Conflict of Interest: The authors declare no competing financial interest.

Acknowledgment. We acknowledge fruitful discussions with Gotthard Seifert. H.L.Y. thanks Jia Gao and Elton Carvalho for communications on the preparation of helically wrapped complexes. This work was partially funded by the European Union (ERDF) *via* the FP7 project CARbon nanoTube phOtONic devices on silicon (CARTOON) and is supported by Dresden Center for Computational Materials Science (DCCMS). We also acknowledge the support by the German Research Foundation (DFG) within the Cluster of Excellence "Center for Advancing Electronics Dresden" (cfAED). We acknowledge the Center for Information Services and High Performance Computing (ZIH) at TU Dresden for computational resources.

Supporting Information Available: The Supporting Information is available free of charge on the ACS Publications website at DOI: 10.1021/acsnano.5b03051.

Calibration of CHARMM force field parameters, stability of the helically wrapped configurations for PFO on CNTs, the determination of the surface coverage of CNT by PFO, variation of the binding energy of PFO−CNT complexes with CNT diameter, the population distributions of HiPco[16] and PLV[19] CNTs with respect to the diameter, the effect of solvent on the adsorption configurations, and the influence of entropic effect on diameter selectivity (PDF)
Movie S1 (MPG)
Movie S2 (MPG)
Movie S3 (MPG)
Movie S4 (MPG)

REFERENCES AND NOTES

1. Saito, R.; Dresselhaus, G.; Dresselhaus, M. S. *Physical Properties of Carbon Nanotubes*; Imperial College Press: London, 1998.
2. Chen, Z.; Appenzeller, J.; Knoch, J.; Lin, Y.-m.; Avouris, P. The Role of Metal-Nanotube Contact in the Performance of Carbon Nanotube Field-Effect Transistors. *Nano Lett.* **2005**, *5*, 1497–502.
3. Lee, H. W.; Yoon, Y.; Park, S.; Oh, J. H.; Hong, S.; Liyanage, L. S.; Wang, H.; Morishita, S.; Patil, N.; Park, Y. J.; et al. Selective Dispersion of High Purity Semiconducting Single-walled Carbon Nanotubes with Regioregular Poly(3-alkylthiophene)s. *Nat. Commun.* **2011**, *2*, 541.
4. Bisri, S. Z.; Gao, J.; Derenskyi, V.; Gomulya, W.; Iezhokin, I.; Gordiichuk, P.; Herrmann, A.; Loi, M. A. High Performance Ambipolar Field-Effect Transistor of Random Network Carbon Nanotubes. *Adv. Mater.* **2012**, *24*, 6147–6152.
5. Sangwan, V. K.; Ortiz, R. P.; Alaboson, J. M. P.; Emery, J. D.; Bedzyk, M. J.; Lauhon, L. J.; Marks, T. J.; Hersam, M. C. Fundamental Performance Limits of Carbon Nanotube Thin-Film Transistors Achieved Using Hybrid Molecular Dielectrics. *ACS Nano* **2012**, *6*, 7480–7488.
6. Ding, J.; Li, Z.; Lefebvre, J.; Cheng, F.; Dubey, G.; Zou, S.; Finnie, P.; Hrdina, A.; Scoles, L.; Lopinski, G. P.; et al. Enrichment of Large-diameter Semiconducting CNTs by Polyfluorene Extraction for High Network Density Thin Film Transistors. *Nanoscale* **2014**, *6*, 2328–39.
7. Brady, G. J.; Joo, Y.; Roy, S. S.; Gopalan, P.; Arnold, M. S. High Performance Transistors *via* Aligned Polyfluorene-sorted Carbon Nanotubes. *Appl. Phys. Lett.* **2014**, *104*, 083107.
8. Bindl, D. J.; Wu, M.-Y.; Prehn, F. C.; Arnold, M. S. Efficiently Harvesting Excitons from Electronic Type-Controlled Semiconducting Carbon Nanotube Films. *Nano Lett.* **2011**, *11*, 455–460.
9. Holt, J. M.; Ferguson, A. J.; Kopidakis, N.; Larsen, B. A.; Bult, J.; Rumbles, G.; Blackburn, J. L. Prolonging Charge Separation in P3HT-SWNT Composites Using Highly Enriched Semiconducting Nanotubes. *Nano Lett.* **2010**, *10*, 4627–4633.
10. See for instance Ding, L.; Tselev, A.; Wang, J.; Yuan, D.; Chu, H.; McNicholas, T. P.; Li, Y.; Liu, J. Selective Growth of Well-Aligned Semiconducting Single-Walled Carbon Nanotubes. *Nano Lett.* **2009**, *9*, 800–805.
11. Sanchez-Valencia, J. R.; Dienel, T.; Groning, O.; Shorubalko, I.; Mueller, A.; Jansen, M.; Amsharov, K.; Ruffieux, P.; Fasel, R. Controlled Synthesis of Single-Chirality Carbon Nanotubes. *Nature* **2014**, *512*, 61–64.
12. Hersam, M. C. Progress Towards Monodisperse Single-Walled Carbon Nanotubes. *Nat. Nanotechnol.* **2008**, *3*, 387–394 and references therein.
13. Star, A.; Stoddart, J. F.; Steuerman, D.; Diehl, M.; Boukai, A.; Wong, E. W.; Yang, X.; Chung, S. W.; Choi, H.; Heath, J. R. Preparation and Properties of Polymer-Wrapped Single-Walled Carbon Nanotubes. *Angew. Chem., Int. Ed.* **2001**, *40*, 1721–1725.
14. OConnell, M. J.; Boul, P.; Ericson, L. M.; Huffman, C.; Wang, Y. H.; Haroz, E.; Kuper, C.; Tour, J.; Ausman, K. D.; Smalley, R. E. Reversible Water-Solubilization of Single-Walled Carbon Nanotubes by Polymer Wrapping. *Chem. Phys. Lett.* **2001**, *342*, 265–271.
15. Nish, A.; Hwang, J. Y.; Doig, J.; Nicholas, R. J. Highly Selective Dispersion of Single-Walled Carbon Nanotubes Using Aromatic Polymers. *Nat. Nanotechnol.* **2007**, *2*, 640–646.
16. Chen, F.; Wang, B.; Chen, Y.; Li, L.-J. Toward the Extraction of Single Species of Single-Walled Carbon Nanotubes Using Fluorene-Based Polymers. *Nano Lett.* **2007**, *7*, 3013–3017.
17. Gao, J.; Loi, M. A.; de Carvalho, E. J. F.; dos Santos, M. C. Selective Wrapping and Supramolecular Structures of Polyfluorene-carbon nanotube Hybrids. *ACS Nano* **2011**, *5*, 3993–3999.
18. Ozawa, H.; Fujigaya, T.; Niidome, Y.; Hotta, N.; Fujiki, M.; Nakashima, N. Rational Concept To Recognize/Extract Single-Walled CarbonNanotubes with a Specific Chirality. *J. Am. Chem. Soc.* **2011**, *133*, 2651–2657.
19. Tange, M.; Okazaki, T.; Iijima, S. Selective Extraction of Semiconducting Single-Wall Carbon Nanotubes by Poly(9.9-dioctylfluorene-alt-pyridine) for 1.5 μm Emission. *ACS Appl. Mater. Interfaces* **2012**, *4*, 6458–6462.
20. Gomulya, W.; Costanzo, G. D.; de Carvalho, E. J. F.; Bisri, S. Z.; Derenskyi, V.; Fritsch, M.; Fröhlich, N.; Allard, S.; Gordiichuk, P.; Herrmann, A.; et al. Semiconducting Single-Walled Carbon Nanotubes on Demand by Polymer Wrapping. *Adv. Mater.* **2013**, *25*, 2948–2956.
21. Mistry, K. S.; Larsen, B. A.; Blackburn, J. L. High-Yield Dispersions of Large-Diameter Semiconducting Single-Walled Carbon Nanotubes with Tunable Narrow Chirality Distributions. *ACS Nano* **2013**, *7*, 2231–2239.
22. Berton, N.; Lemasson, F.; Poschlad, A.; Meded, V.; Tristram, F.; Wenzel, W.; Hennrich, H.; Kappes, M. M.; Mayor, M. Selective Dispersion of Large-Diameter Semiconducting Single-Walled Carbon Nanotubes with Pyridine-Containing Copolymers. *Small* **2014**, *10*, 360–367.
23. Fukumaru, T.; Toshimitsu, F.; Fujigaya, T.; Nakashima, N. Effects of the Chemical Structure of Polyfluorene on Selective Extraction of Semiconducting Single-walled Carbon Nanotubes. *Nanoscale* **2014**, *6*, 5879–86.
24. Avouris, Ph.; Freitag, M.; Perebeinos, V. Carbon-Nanotube Photonics and Optoelectronics. *Nat. Photonics* **2008**, *2*, 341–350.
25. Zheng, M.; Jagota, A.; Semke, E. D.; Diner, B. A.; Mclean, R. S.; Lustig, S. R.; Richardson, R. E.; Tassi, N. G. DNA-Assisted Dispersion and Separation of Carbon Nanotubes. *Nat. Mater.* **2003**, *2*, 338–342.
26. Chen, J.; Liu, H. Y.; Weimer, W. A.; Halls, M. D.; Waldeck, D. H.; Walker, G. C. Noncovalent Engineering of Carbon Nanotube Surfaces by Rigid, Functional Conjugated Polymers. *J. Am. Chem. Soc.* **2002**, *124*, 9034–9035.
27. Kang, Y. K.; Lee, O.; Deria, P.; Kim, S. H.; Park, T.; Bonnell, D. A.; Saven, J. G.; Therien, M. J. Helical Wrapping of Single-Walled Carbon Nanotubes by Water Soluble Poly(p-phenyleneethynylene). *Nano Lett.* **2009**, *9*, 1414–1418.

28. Giulianini, M.; Waclawik, E. R.; Bell, J. M.; de Crescenzi, M.; Castrucci, P.; Scarselli, M.; Motta, N. Regioregular Poly(3-hexyl-thiophene) Helical Self-organization on Carbon Nanotubes. *Appl. Phys. Lett.* **2009**, *95*, 013304.
29. White, C. T.; Robertson, D. H.; Mintmire, J. W. Helical and Rotational Symmetries of Nanoscale Graphitic Tubules. *Phys. Rev. B: Condens. Matter Mater. Phys.* **1993**, *47*, 5485–89.
30. Mason, T. J.; Lorimer, J. P. *Sonochemistry: Theory, Applications and Use of Ultrasound in Chemistry*; Ellis Horwood: New York, 1989.
31. Huang, Y. Y.; Terentjev, E. M. Dispersion of Carbon Nanotubes: Mixing, Sonication, Stabilization, and Composite Properties. *Polymers* **2012**, *4*, 275–295.
32. Justino, L. L. G.; Ramos, M. L.; Knaapila, M.; Marques, A. T.; Kudla, C. J.; Scherf, U.; Almasy, L.; Schweins, R.; Burrows, H. D.; Monkman, A. P. Gel Formation and Interpolymer Alkyl Chain Interactions with Poly(9,9-dioctylfluorene-2,7-diyl) (PFO) in Toluene Solution: Results from NMR, SANS, DFT, and Semiempirical Calculations and Their Implications for PFO β-Phase Formation. *Macromolecules* **2011**, *44*, 334–343.
33. Shea, M. J.; Mehlenbacher, R. D.; Zanni, M. T.; Arnold, M. S. Experimental Measurement of the Binding Configuration and Coverage of Chirality-Sorting Polyfluorenes on Carbon Nanotubes. *J. Phys. Chem. Lett.* **2014**, *5*, 3742–3749.
34. Further details can be found in the Supporting Information.
35. Wang, H.; Koleilat, G. I.; Liu, P.; Jiménez-Osés, G.; Lai, Y.; Vosgueritchian, M.; Fang, Y.; Park, S.; Houk, K. N.; Bao, Z. High-Yield Sorting of Small-Diameter Carbon Nanotubes for Solar Cells and Transistors. *ACS Nano* **2014**, *8*, 2609–2617.
36. Nicolosi, V.; Chhowalla, M.; Kanatzidis, M. G.; Strano, M. S.; Coleman, J. N. Liquid Exfoliation of Layered Materials. *Science* **2013**, *340*, 1226419.
37. Kolmogorov, A. N.; Crespi, V. H. Registry-Dependent Interlayer Potential for Graphitic Systems. *Phys. Rev. B: Condens. Matter Mater. Phys.* **2005**, *71*, 235415.
38. Hwang, J.-Y.; Nish, A.; Doig, J.; Douven, S.; Chen, C.-W.; Chen, L.-C.; Nicholas, R. J. Helical Wrapping of Single-Walled Carbon Nanotubes by Water Soluble Poly(p-phenyleneethynylene). *J. Am. Chem. Soc.* **2008**, *130*, 3543–3553.
39. Vanommeslaeghe, K.; Hatcher, E.; Acharya, C.; Kundu, S.; Zhong, S.; Shim, J.; Darian, E.; Guvench, O.; Lopes, P.; Vorobyov, I.; et al. CHARMM General Force Field (CGenFF): A Force Field for Drug-like Molecules Compatible with the CHARMM All-atom Additive Biological Force Fields. *J. Comput. Chem.* **2010**, *31*, 671–690.
40. Pronk, S.; Páll, S.; Schulz, R.; Larsson, P.; Bjelkmar, P.; Apostolov, R.; Shirts, M. R.; Smith, J. C.; Kasson, P. M.; van der Spoel, D. GROMACS 4.5: A High-throughput and Highly Parallel Open Source Molecular Simulation Toolkit. *Bioinformatics* **2013**, *29*, 845–854.
41. Allinger, N. L.; Yuh, Y. H.; Lii, J. H. Molecular Mechanics. The MM3 Force Field for Hydrocarbons. *J. Am. Chem. Soc.* **1989**, *111*, 8551–8566.
42. *TINKER 6.3*, executables and source at http://dasher.wustl.edu/tinker/.
43. Lippert, G.; Hutter, J.; Parrinello, M. A Hybrid Gaussian and Plane Wave Density Functional Scheme. *Mol. Phys.* **1997**, *92*, 477–487.
44. Grimme, S.; Antony, J.; Ehrlich, S.; Krieg, H. A Consistent and Accurate ab initio Parametrization of Density Functional Dispersion Correction (DFT-D) for the 94 Elements H-Pu. *J. Chem. Phys.* **2010**, *132*, 154104.
45. Becke, A. D. Density-functional Exchange-energy Approximation with Correct Asymptotic Behavior. *Phys. Rev. A: At., Mol., Opt. Phys.* **1988**, *38*, 3098. Lee, C.; Yang, W.; Parr, R. G. Develop- ment of the Colle-Salvetti correlation-energy formula into a functional of the electron density. *Phys. Rev. B: Condens. Matter Mater. Phys.* **1988**, *37*, 785.
46. Berton, N.; Lemasson, F.; Hennrich, F.; Kappes, M. M.; Mayor, M. Influence of Molecular Weight on Selective Oligomer-assisted Dispersion of Single-walled Carbon Nanotubes and Subsequent Polymer Exchange. *Chem. Commun.* **2012**, *48*, 2516–2518.
47. Tu, X.; Manohar, S.; Jagota, A.; Zheng, M. DNA Sequence Motifs for Structure-specific Recognition and Separation of Carbon Nanotubes. *Nature* **2009**, *460*, 250–253.
48. Von Bargen, C. D.; MacDermaid, C. M.; Lee, O.-S.; Deria, P.; Therien, M. J.; Saven, J. G. Origins of the Helical Wrapping of Phenyleneethynylene Polymers about Single-Walled Carbon Nanotubes. *J. Phys. Chem. B* **2013**, *117*, 12953–12965.
49. Ju, S.-Y.; Doll, J.; Sharma, I.; Papadimitrakopoulos, F. Seletion of Carbon Nanotubes with Specific Chiralities Using Helical Assemblies of Flavin Mononucleotide. *Nat. Nanotechnol.* **2008**, *3*, 356–362.
50. Johnson, R. R.; Johnson, A. T.; Klein, M. L. Probing the structure of DNA-Carbon Nanotube Hybrids with Molecular Dynamics. *Nano Lett.* **2008**, *8*, 69–75.